Korean J. Chem. Eng., **29**(6), 743-749 (2012)
DOI: 10.1007/s11814-011-0237-8

The examination of surface chemistry and porosity of carbon nanostructured adsorbents for 1-naphthol removal from petrochemical wastewater streams

Mansoor Anbia† and Seyyed Ershad Moradi

Research Laboratory of Nanoporous Materials, Faculty of Chemistry,
Iran University of Science and Technology, Narmak, Tehran 16846, Iran
(*Received 6 June 2011 • accepted 9 September 2011*)

Abstract–Chemically modified mesoporous carbon (CMMC) and chemically modified activated carbon (CMAC) were prepared by an acid surface modification method from mesoporous carbon (MC) and commercial activated carbon (AC) by wet impregnation method. The structural order and textural properties of the nanoporous materials were studied by XRD and nitrogen adsorption. The presence of carboxylic functional groups on the carbon surface was confirmed by FTIR analyses. Adsorption of 1-naphthol over various porous adsorbents such as CMMC, CMAC, MC and AC was studied. The adsorption isotherms of 1-naphthol were in agreement with a Langmuir model; moreover, the uptake capacity of 1-naphthol followed the order: CMMC>MC>CMAC>AC.

Key words: 1-Naphthol, Chemical Modification, Activated Carbon, Adsorption, Langmuir Isotherm, Nanoporous

INTRODUCTION

Polycyclic aromatic hydrocarbons (PAHs), which are chemical species with two to six fused benzene rings, are well known toxic hazardous pollutants and highly potent carcinogens that can cause tumors in some organisms [1]. In recent years, PAHs contamination in water systems has drawn increasing attention. PAHs originate from natural and anthropogenic sources that include engine exhaust, industrial processes, crude oil, urban run-off, domestic heating systems, incinerators and smoke. Natural sources include terrestrial coal deposits, volcanic eruptions and forest fires. The main sources of PAHs in surface water are atmospheric deposition, runoff from contaminated soils and deposition from sewage discharges [2]. Most PAHs are hydrophobic with high boiling and melting points and electrochemical stability. Therefore, they can exist and be accumulated in soils or water for a long time [3].

Adsorption treatment provides a simple and universal approach to effectively removing organic pollutants from the aquatic environment. The removal of toxic organic pollutants from water is a problem, particularly when they are present in low concentrations. Several studies have focused on the fate and transport of these pollutants and the application of remedial technologies to manage them [4-10]. Activated carbons present an outstanding adsorption capacity that stems from their high surface area, pore structure and surface chemical properties. These materials are effective adsorbents for priority pollutants, therefore being suitable for the decontamination of water and wastewater. These porous carbons are generally microporous, and the preparation of carbon materials with well ordered mesoporous structure would offer many application possibilities not only in the adsorption and separation of large molecules whose molecular sizes are too large to enter micropores but also in electrical double layer capacitors, gas separation, catalysis, water and air purification and energy storage. Recently, Ryoo et al. prepared ordered mesoporous carbons from mesoporous silica templates such as MCM-48, SBA-1 and SBA-15 using sucrose as the carbon source [11-14].

Adsorption plays an important role in these processes. Therefore, the interactions of such compounds with the mesoporous carbon surface must be studied in detail. The mesoporous carbon materials adsorption capacity depends on quite different factors. Obviously, it depends on the mesoporous carbon's characteristics: texture (surface area, pore size distributions), surface chemistry (surface functional groups) [15-17]. It also depends on adsorptive characteristics: molecular weight, polarity, pK_a, molecular size, and functional groups. The influence of the texture and surface chemistry of nanoporous carbons in the adsorption of organic compounds has been studied for years, and many references on this topic can be found in the literature. The adsorption of organic molecules from aqueous solutions on nanoporous carbons has been recently reviewed [18,19], and it was shown that the specific mechanism by which the adsorption of many organic compounds takes place on this adsorbent is still ambiguous. Since the pioneering works of Coughlin and Ezra [20] and Mattson et al. [21] to others published more recently [22-25], it was found that the adsorption capacity is significantly affected by the carbonaceous adsorbent surface chemistry.

Different studies have been done on the interaction between acid oxygen-containing surface groups and the adsorption of organic compounds in aqueous solution. There are two types of interactions between the adsorbate and the carbonaceous adsorbent: electrostatic and dispersive [17-19]. The former appears when the adsorptive is dissociated under the experimental conditions used; for the latter, three mechanisms are proposed: π-π dispersion interaction mechanism, the hydrogen bonding formation mechanism, and the electron donor-acceptor complex mechanism. The π-π dispersion interaction mechanism is the most widely accepted [17,18]. The surface chemistry and solution pH are the most important factors controlling the adsorption process [26]. Most of the aromatic pollutants

†To whom correspondence should be addressed.
E-mail: anbia@iust.ac.ir

are found in water solution in the molecular state for a broad range of pH values. In this case, dispersive interactions are predominant, mainly because of the attraction between the π orbitals on the carbon basal planes and the electronic density in the adsorbate aromatic rings (π-π interactions). However, when the solution pH is very high or very low, ions may be present, so electrostatic interaction between them and charged functional groups on the carbon surface could be significant [17].

In this work, the influence of the texture and surface chemistry of nanoporous carbon adsorbent were systematically studied in the adsorption of 1-naphthol (NA). For this purpose, mesoporous carbon and commercial activated carbon with quite different textural properties were selected in order to analyze the influence of the textural parameters. Then both of them were modified by selected oxidative treatments, producing samples differing in the surface chemistry and textural parameters, to study their influence in the adsorption process. Interestingly, it has been found that the adsorption capability of chemically modified mesoporous carbon for 1-naphthol is much higher compared to that of other adsorbents. Langmuir and Freundlich adsorption isotherms were studied to explain the sorption mechanism.

EXPERIMENTAL

1. Materials

The reactants used in this study were synthesized mesoporous silica (MCM-48) and sucrose as a carbon source, sulfuric acid as a catalyst for synthesis of mesoporous carbon and nitric acid as a oxidizer agent, 1-naphthol and commercial activated carbon. All the chemicals were of analytical grade and purchased from Merck.

2. Synthesis of Mesoporous Carbon (MC)

High-quality MCM-48 sample was prepared following the synthesis procedure reported by Shao et al. [27]. Then 1.25 g sucrose and 0.14 g H_2SO_4 in 5.0 g H_2O were dissolved, and this solution was added to 1 g MCM-48. The sucrose solution corresponded approximately to the maximum amount of sucrose and sulfuric acid that could be contained in the pores of 1 g MCM-48. The resultant mixture was dried in an oven at 373 K, and subsequently, the oven temperature was increased to 433 K. After 6 h at 433 K, the MCM-48 silica containing the partially carbonizing organic masses was added to an aqueous solution consisting of 0.75 g sucrose, 0.08 g H_2SO_4 and 5.0 g H_2O. The resultant mixture was dried again at 373 K, and subsequently the oven temperature was increased to 433 K. The sample turned very dark brown or nearly black. This powder sample was heated to 1,173 K under vacuum using a fused quartz reactor equipped with a fritted disk. The carbon-silica composite thus obtained was washed with 1 M NaOH solution of 50% ethanol-50% H_2O twice at 363 K, in order to dissolve the silica template completely. The carbon samples obtained after the silica removal were filtered, washed with ethanol and dried at 393 K.

3. Chemical Modification of MC and Commercial Activated Carbon

To introduce oxygen-containing functional groups on the carbon surface, MC (or commercial activated carbon) was oxidized by nitric acid under optimal modification condition, such as nitric acid concentration, oxidation temperature [28]. 0.1 g of dried MC (or commercial activated carbon) powder was treated with 15 ml of HNO_3 solution (2 M solution) for 1 h in the 80 °C under refluxing. After oxidation, samples were recovered and washed thoroughly with distilled water until the pH was close to 7.

4. Characterization

The X-ray powder diffraction patterns were recorded on a Philips 1830 diffractometer using Cu Kα radiation. The diffractograms were recorded in the 2θ range of 0.8-10 with a 2θ step size of 0.01° and a step time of 1 s. Adsorption-desorption isotherms of the synthesized samples were measured at 77 K on Micromeritics model ASAP 2010 sorptometer to determine an average pore diameter. Pore-size distributions were calculated by the Barrett-Joyner-Halenda (BJH) method, while surface area of the sample was measured by Brunauer-Emmet-Teller (BET) method. The Fourier transform infrared spectra for the unmodified and modified samples were measured on a DIGILAB FTS 7000 instrument under attenuated total reflection (ATR) mode using a diamond module.

5. Adsorption Studies

A stock solution of 50 ppm for 1-naphthol (NA) was prepared by dissolving an appropriate amount of the 1-naphthol in ultra-pure water (18 MΩ cm) derived from a Milli-Q plus 185 water purifier. Batch adsorption isotherms were performed by shaking 500 ml amber Winchester bottles containing the required concentration of the 1-naphthol in a Gallenkamp incubator shaker. The shaker was set at a temperature of 298±1 K and a speed of 200 rpm. Initial solution concentration of 0-0.14 mmol/L was prepared by pipetting out the required amounts of the 1-naphthol from the stock solution. The volume of solution in each bottle was maintained at 500 mL and the solutions were adjusted to pH 5. About 5 mg of each adsorbent was weighed accurately on aluminum foils using a Sartorious (Model BP 201D) analytical balance. The adsorbents were transferred carefully into the bottles using 10 mL solutions from the bottles. The bottles were shaken vigorously before shaking for different time in the incubator shaker (New Brunswick Scientific C25 Model).

The amount of 1-naphthol adsorbed was calculated by subtracting the amount found in the supernatant liquid after adsorption from the amount of 1-naphthol present before addition of the adsorbent by UV-Vis spectrophotometer (UV mini 1240 Shimadzu). Absorbance was measured at wavelength (λ_{max}) 331 nm for determination of 1-naphthol content. Calibration experiments were done separately before each set of measurements with 1-naphthol's solution of different concentrations. Centrifugation prior to the analysis was used to avoid potential interference from suspended scattering particles in the UV-Vis analysis.

The adsorption capacities were calculated based on the differences of the concentrations of solutes before and after the experiment according to Eq. (1) [29].

$$q_e = \frac{(C_o - C_e)V}{W} \quad (1)$$

Where q_e is the concentration of the adsorbed solute (mmol/g); C_o and C_e are the initial and final (equilibrium) concentrations of the solute in solution (mmol/L); V (mL) is the volume of the solution and W (g) is the mass of the adsorbent.

6. Adsorption Kinetics of 1-Naphthol (NA)

$$q_t = \frac{(C_o - C_t)V}{W} \quad (2)$$

For the measurement of the time resolved uptake of 1-naphthol onto adsorbents, 15 ml of distilled water was mixed with 60 mg of MC (or activated carbon) in a 500 ml flask for about 10 min. 285 ml of 1-naphthol solution was quickly introduced into the flask (keeping the initial concentrations of the resulting solutions at 50 ppm) and stirred continuously at 20 °C. Samplings were done by fast filtration at different time intervals. The concentration of residual 1-naphthol in the solution was determined and the adsorption amount q_t was calculated according to Eq. (2).

Where q_t is the adsorption amount at time t, C_o is the initial concentration of 1-naphthol solution, C_t is the concentration of 1-naphthol solution at time t, and V is the volume of 1-naphthol solution and m is the mass of carbonaceous adsorbent.

RESULTS AND DISCUSSION

1. Characterization of the CMMC and MC Samples

The quality of the mesoporous carbon samples prepared in this study was examined by nitrogen adsorption-desorption analysis and X-ray diffraction (XRD) techniques.

Nitrogen physisorption is the method of choice to gain knowledge about mesoporous materials. This method gives information on the specific surface area and the pore diameter. Calculating pore diameters of mesoporous materials using the BJH method is common. Former studies show that the application of the BJH theory gives appropriate qualitative results, which allow a direct comparison of relative changes between different mesoporous materials.

The nitrogen sorption isotherms of the MC and CMMC have the typical type IV shape. Interestingly, the pore size distributions are essentially the same as before acid oxidation. The adsorption uptakes at relative pressure close to p/p_o=0 are identical (p the equilibrium pressureare and p_o the saturation pressure of adsorbents at the temperature of adsorption). However, the total uptakes are slightly different, decreasing with the surface modification with acid. As shown in Table 1, the decreases in the specific surface areas and pore volumes are 2.5% and 9.5%, respectively. From the nitrogen sorption isotherms (Fig. 1) of mesoporous carbon type carbons before and after acid oxidation, it can be seen that after oxidation the obtained carbons still have type IV isotherms, indicating that mesoporosity is still preserved. However, the oxidation leads to a decrease in the total uptake of the oxidized carbons, which reflects the decrease of the total pore volume resulting from acid oxidation. Interestingly, the oxidized carbons essentially keep the bimodal pore size distribution, which is characteristic of the parent MC. The textural parameters listed in Table 1 clearly confirm the structural changes of oxidized MC. Especially, the variations of the surface area and pore volume are significant with the increase in the acid concentration.

Table 1. Textural parameters of the MC and CMMC employed in this study

Adsorbent	d spacing (nm)	A_{BET} (m^2 g^{-1})	V_p (cm^3 g^{-1})
MC	3.4	1010.5	0.69
CMMC	3.1	985.4	0.62

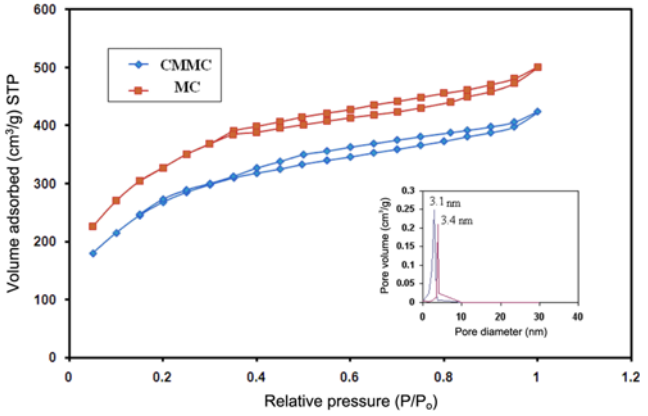

Fig. 1. Adsorption-desorption isotherms of nitrogen at 77 K on MC and CMMC. The insert shows the BJH pore size distribution calculated from the desorption branch of the isotherm.

To check the structural degradation, XRD data of CMMC and MC were obtained on Philips 1830 diffractometer using Cu Kα radiation of wavelength 0.154 nm. Fig. 2 shows the XRD peaks of the samples. The XRD patterns of CMMC showed three diffraction peaks that can be indexed to (110), (210), and (220) in the 2θ range from 0.8° to 10°, representing well-ordered cubic pores [11].

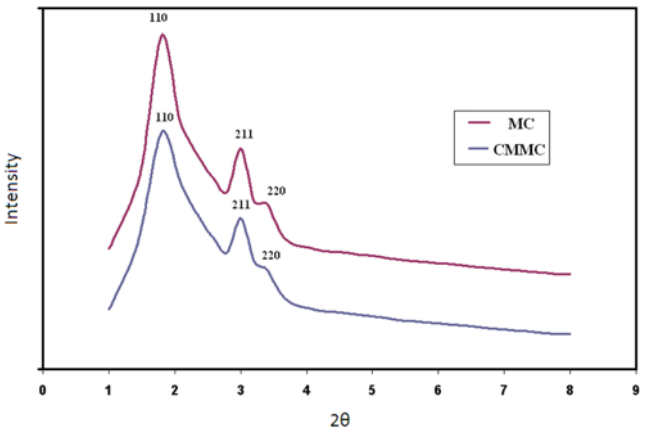

Fig. 2. XRD pattern of CMMC and MC.

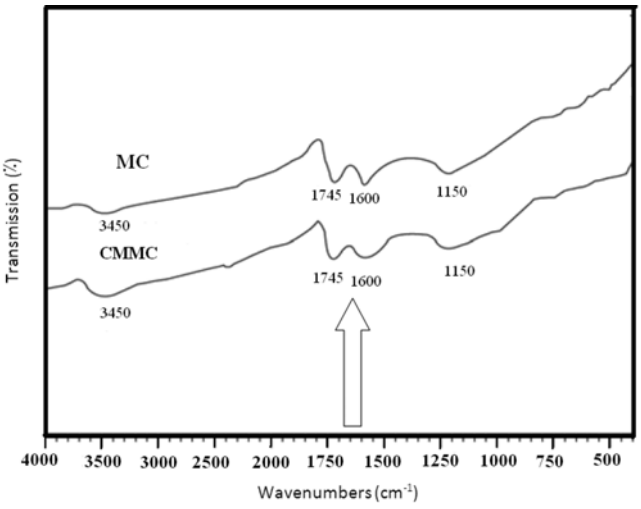

Fig. 3. FT-IR spectra of MC and CMMC samples.

The XRD patterns of MC carbon and CMMC (in Fig. 2) show well-resolved reflections indicating that MC carbon nicely maintains it original structure even after the oxidization with 2 M nitric acid. For CMMC sample, the cubic structure of MC was maintained well, but the XRD reflections become less pronounced, which might be due to the partial damage of the mesoporous (cubic) structure or due to the decreased contrast between walls and pores because of the cleavage of the carbon species from the pore walls.

The FT-IR technique was used to monitor changes on the surface of the mesoporous carbon and the content of the introduced oxygen-containing functional surface group [6,7]. Fig. 3 shows the FT-IR spectra of MC and as treated CMMC samples. A broad band at around 3,450 cm^{-1} was observed in all samples. The O-H stretching vibration of the adsorbed water molecules, which also had a bending vibration mode corresponding to the band recorded at 1,630 cm^{-1}, mainly caused it. Bands at 1,643-1,750 cm^{-1} denoted the absorption of stretching and bending vibration modes of -COOH on the surface of mesoporous carbon materials (indicated by arrow). In addition, the stretching vibration of C-O bonds caused the broad band that appeared at 1,100 cm^{-1}. The relative intensity of these bands in CMMC samples was higher than those of the MC sample, indicating that more oxygen-containing functional groups were introduced when the oxidation was done. This fact, that oxidation caused higher content of functional groups, indicated that there were chemical reactions on the carbon surface between the nitric acid and C atoms, which were partially oxidized to form C-OH and/or -COOH. The reaction equations were proposed as follows:

-C-oxidize-C-OH
-C-oxidize-C-OOH

2. Characterization of the CMAC and AC Samples

The nitrogen adsorption isotherms of activated carbon samples are shown in Fig. 4. The N_2 adsorption isotherms are all type I even though their shape varies significantly, indicative of microporous carbons. Some previous works for different activated carbons [30-33] have observed similar isotherms. The adsorption isotherm of CMAC is typical for highly microporous carbon, with a very steep initial uptake and a relative absence of meso- and macroporosity; however, sample AC reached adsorption saturation at lower P/P_o.

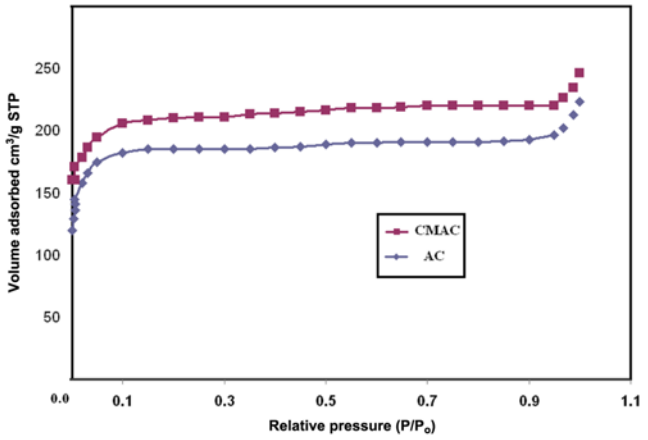

Fig. 4. Adsorption-desorption isotherms of nitrogen at 77 K on AC and CMAC.

Table 2. Textural parameters of the AC and CMAC employed in this study

Adsorbent	d Spacing (nm)	A_{BET} (m^2 g^{-1})	V_p (cm^3 g^{-1})
AC	2.16	936	0.41
CMAC	2.09	1209	0.59

In addition, the adsorption ability of CMAC is higher than AC according to the higher position of isotherm curve, as shown in Fig. 4. Some porous structure parameters of the activated carbons are shown in Table 2. The results show that chemical modification prior to activation dramatically increased the BET surface area and total pore volume V_t (estimated from the liquid volume of nitrogen adsorbed at relative pressure P/P_0=0.996) of the resulting activated carbon. This is a result of more 'active site' by the formation of oxygen groups, which makes it easier for acid to react with the carbon of the precursor, and finally developed the porous structure.

The XRD analysis was carried out on powder samples to investigate the structural changes. The typical XRD patterns of the activated carbons and their precursors are shown in Fig. 5. As shown in Fig. 5, the XRD result is not very clear, but something, which is very important, is the overall changes in XRD result. It can be clearly seen that there are diffraction peaks around 2θ=25^0 for AC, corre-

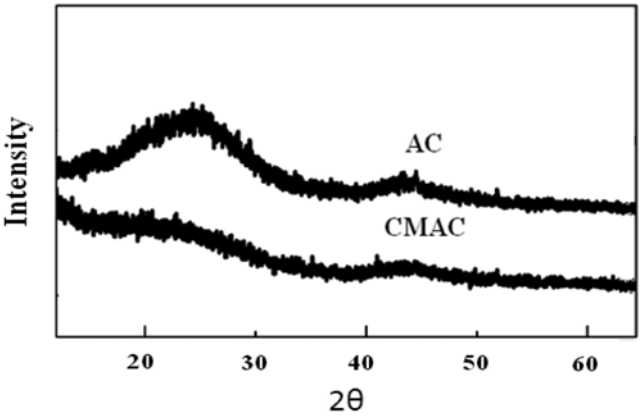

Fig. 5. XRD analysis of the activated carbons and chemical modified activated carbon.

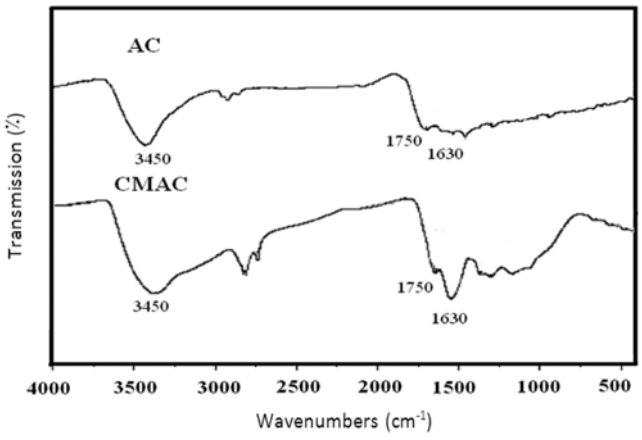

Fig. 6. FT-IR spectra of AC and CMAC samples.

sponding to the diffraction of (002). The (002) peak of AC is broader and the (002) peak of CMAC disappeared.

In the FTIR spectra (Fig. 6) of the AC and CMAC tested, the band of O-H stretching vibrations (3,600-3,100 cm^{-1}) was due to surface hydroxylic groups and chemisorbed water. The asymmetry of this band at lower wave numbers indicates the presence of strong hydrogen bonds. Below 2,000 cm^{-1}, the FTIR spectra of activated carbon (AC) exhibit absorption typical of surface functional groups and component oxygen species of the structural network. These spectra are similar to those reported of other carbons derived from a wide variety of sources [34-37]. The presence of bands at 1,750 cm^{-1} and 1,630 cm^{-1} can be, respectively, attributed to the stretching vibrations of C=O moieties in carboxylic or ester and quinine structures [36]. Since H_2O is sorbed on the surface of OH bending vibrations can also describe activated carbons with the participation of specific (hydrogen bonds, chemisorptions due to surface oxide hydration) and non-specific interactions (physical adsorption), the bands in the 1,500-1,600 cm^{-1} region. The complicated nature of the adsorption bands in the 1,650-1,500 cm^{-1} region suggests that aromatic ring bands and double bond (C=C) vibrations overlap the aforementioned C=O stretching vibration bands and OH deformation bands [36]. After oxidation, the band characteristic of carbonyl moieties in a carboxylic acid (1,750-1,700 cm^{-1}) increases and there is a simultaneous, considerable increase in band intensity of these carbonyl functional groups in different surroundings. This suggests an increase in the number of ether and hydroxylic structures in the carbon investigated.

3. Adsorption Studies

3-1. Effect of Agitation Speed

The effect of agitation speed on removal efficiency of 1-naphthol on carbonaceous adsorbents was studied by varying the speed of agitation from 50 to 250 rpm, while keeping the analyte concentration, contact time, pH, temperature and dose of the adsorbent as constant. As it is demonstrated in Fig. 7, the 1-naphthol removal efficient generally increased with increasing agitation speed from 50 rpm to 150 rpm and the adsorption capacity of all adsorbents remained constant for agitation rates greater than 150 rpm. These results can be associated with the fact that the increase of the agitation speed improves the diffusion of analyte into the pores of the adsorbents. This also indicates that a shaking rate in the range 150-200 rpm is sufficient to assure that the maximum available sites of adsorbent existing in the pores of adsorbents are made readily available for 1-naphthol uptakes. For convenience, agitation speed of 150 rpm was selected as the optimum speed for all the adsorption experiments.

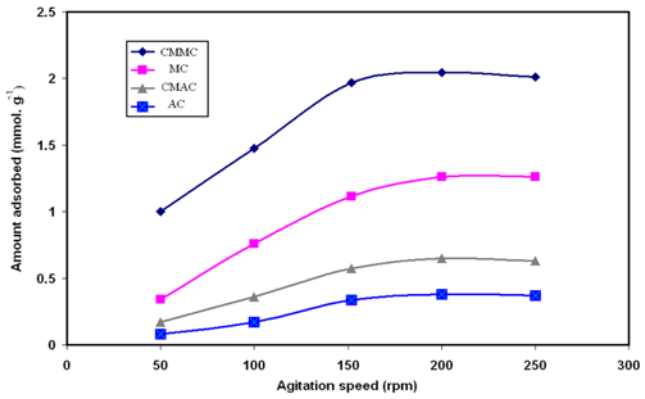

Fig. 7. Effect of agitation speed on the adsorption capacity of adsorbents (adsorbents dosage=0.2 g/L, [NA]=50 ppm, contact time=4 h, T=298 K and pH=7).

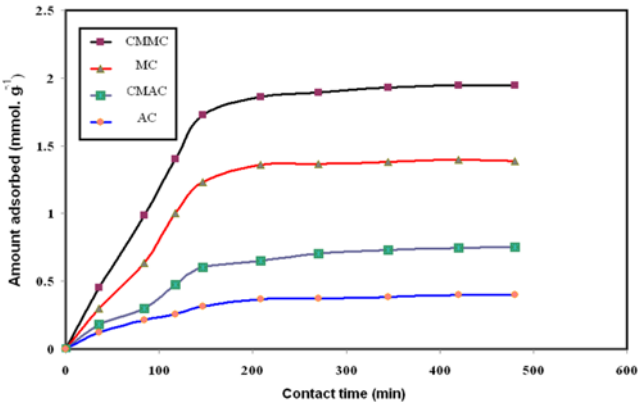

Fig. 8. Effect of contact time on removal of 1-naphthol ([NA]=50 mg/L, agitation speed=150 (rpm), adsorbent dosage=0.2 g/L, T=298 K and pH=7).

3-2. Effect of Contact Time and Concentration

To establish equilibration time for maximum uptake and to know the kinetics of adsorption process, the adsorption of 1-naphthol on carbonaceous adsorbent was studied as a function of contact time, and results are shown in Fig. 8. It is seen that the rate of uptake of the 1-naphthol is rapid in the beginning and 50% adsorption is completed within 80 min. Fig. 8 also indicates that the time required for equilibrium adsorption is 200 min. Thus, for all equilibrium adsorption studies, the equilibration period was kept 240 min. The effect of concentration on the equilibration time was also investigated as a function of initial 1-naphthol concentration, and the results are shown in Fig. 9 (on MC). It was found that time of equilibrium as well as time required to achieve a definite fraction of equilibrium adsorption is independent of initial concentration. These results indicate that the adsorption process is first order.

3-3. Effect of Chemical Modification

To evaluate the efficacy of the prepared adsorbents, the equilib-

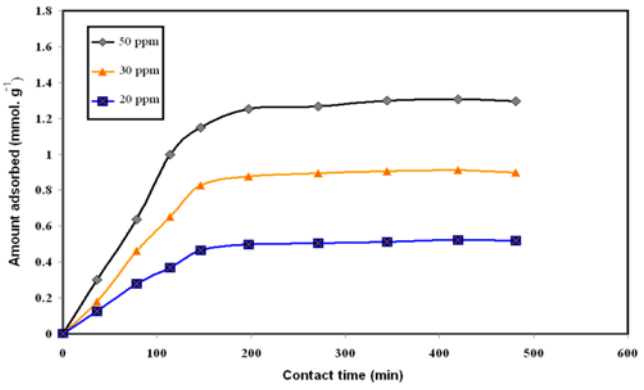

Fig. 9. Effect of initial concentration on removal of 1-naphthol (contact time=4 h, agitation speed=150 (rpm), adsorbent dosage=0.2 g/L, T=298 K and pH=7).

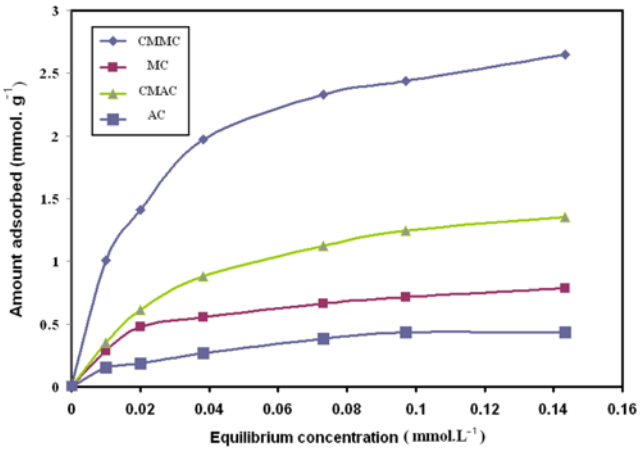

Fig. 10. Adsorption isotherm for 1-naphthol removal on carbonaceous adsorbents (contact time=4 h, agitation speed=150 (rpm), adsorbent dosage=0.2 g/L, T=298 K and pH=7).

rium adsorption of the 1-naphthol was studied as a function of equilibrium concentration. The adsorption isotherms of 1-naphthol on adsorbents are shown in Fig. 10. It is seen that the order of adsorption in terms of amount adsorbed (mmol/g) on different adsorbents is CMMC>MC and CMAC>AC. The higher adsorption capacity of CMMC and CMAC can be explained by several facts. Undoubtedly, increasing in interaction as a cause of more functional group in CMMC and CMAC explained this. It is also surmised that the anchoring ability of -COOH groups located inside and at the entrance of the mesopores might obstruct desorption of PAHs molecules from the pore channels of chemically oxidized mesoporous carbon, resulting in an increase in the PAHs adsorption capacity.

3-4. Langmuir and Freundlich Isotherms

To indicate the sorption behavior and to estimate of adsorption capacity, adsorption isotherms have been studied. The adsorption processes of 1-naphthol were tested with Langmuir and Freundlich isotherm models [38]. Two commonly used empirical adsorption models, Freundlich and Langmuir, which correspond to heterogeneous and homogeneous adsorbent surfaces, respectively, were employed in this study. The Freundlich model is given by Eq. (3):

$$\mathrm{L}nq_e = \ln K_f + \left(\frac{1}{n}\right)\ln C_e \qquad (3)$$

where K_f and n are the Freundlich constants related to adsorption capacity and intensity, respectively. In the second model, the Langmuir equation assumes maximum adsorption occurs when the surface is covered by the adsorbate, because the number of identical sites on the surface is finite. Eq. (4) (Langmuir equation) is given as follows:

$$\frac{C_e}{q_e} = \left(\frac{1}{q_m b}\right) + \left(\frac{1}{q_m}\right)C_e \qquad (4)$$

where q_e (mmol g^{-1}) is the amount adsorbed at equilibrium concentration C_e (mmol L^{-1}), q_m (mg g^{-1}) is the Langmuir constant representing maximum monolayer capacity and b is the Langmuir constant related to energy of adsorption.

The isotherm data have been linearized using the Langmuir equation and Freundlich equation. The regression constants are in Table 3. The value of the correlation coefficients shows that the data conform well to the Langmuir equation.

CONCLUSIONS

Liquid-phase oxidation by nitric acid was used for the surface modification of carbon nanoporous materials. The chemically modified nanoporous carbon prepared in this work is suitable for the adsorption of aqueous 1-naphthol from industrial wastewater. It is indicated that the surface oxygen groups of the precursor could act as 'active site', which plays an important role in adsorption process. The adsorption behavior of 1-naphthol on the carbonaceous adsorbent from aqueous solution has been investigated. All adsorption isotherms were fitted well by Langmuir model.

ACKNOWLEDGEMENTS

The Research Council of Iran University of Science and Technology and Iranian Nanotechnology Initiative Council are acknowledged for the financial support.

REFERENCES

1. R. G. Harvey, *Polycyclic Aromatic Hydrocarbons, Chemistry and Carcinogenicity*, Cambridge University Press, Cambridge, England (1991).
2. D. M. Wassenberg and R. T. Di Giulio, *Environ. Health Perspect.*, **17**, 1658 (2004).
3. C. Chang, C. Y. Chang, K. Chen, W. Tsai, J. Shie and Y. Chen, *J. Colloid Interface Sci.*, **277**, 29 (2004).
4. M. Anbia, M. K. Rofouei and S. W. Husain, *Chin. J. Chem.*, **24**, 1026 (2006).
5. M. Anbia, M. K Rofouei and S. W. Husain, *Oriental J. Chem.*, **21**, 199 (2005).
6. M. Anbia and S. E. Moradi, *Chem. Eng. J.*, **148**, 452 (2008).
7. M. Anbia and S. E. Moradi, *Appl. Surf. Sci.*, **5041**, 255 (2009).
8. M. Hudson, S. W. Husain and M. Anbia, *J. Ir. Chem. Soc.*, **2**, 54

Table 3. Langmuir and Freundlich constants for adsorption of PAHs on CMMC and CMAC

	Langmuir			Freundlich		
Adsorbent	q_m (mmol/g)	b (L/mmol)	R^2	K_F (mmol/g)	n (L/mmol)	R^2
CMMC	3.0	47.14	0.999	5.8	2.75	0.964
MC	1.7	27.85	0.999	4.0	2.00	0.961
CMAC	0.9	49.26	0.996	1.6	2.85	0.937
AC	0.5	30.7	0.983	1.1	2.29	0.971

(2005).
9. N. Tancredi, N. Medero, F. Moller, J. Piriz, C. Plada and T. Cordero, *J. Colloid Interface Sci*., **279**, 357 (2004).
10. Y. Lin and H. Teng, *Carbon*, **41**, 2865 (2003).
11. S. Jun, S. H. Joo, R. Ryoo, M. Kruk, M. Jaroniec, Z. Liu, T. Ohsuna and O. Terasaki, *J. Am. Chem. Soc*., **122**, 10712 (2000).
12. R. Ryoo, S. H. Joo and S. Jun, *J. Phys. Chem. B*., **103**, 7743 (1999).
13. R. Ryoo, S. H. Joo, M. Kruk and M. Jaroniec, *Adv. Mater*., **13**, 677 (2001).
14. S. H. Joo, S. J. Choi, I. Oh, J. Kwak, Z. Liu, O. Terasaki and R. Ryoo, *Nature*, **412**, 169 (2001).
15. R. C. Bansal, J. Donnet and H. F. Stoeckli, Active Carbon, Dekker, New York (1988).
16. S. J. Gregg and K. S. W. Sing, Adsorption, Surface Area and Porosity, Academic Press, London (1982).
17. L. R. Radovic, I. F. Silva, J. I. Ume, J. A. Menéndez, C. A. Leon and A. W. Scaroni, *Carbon*, **35**, 1339 (1997).
18. L. R. Radovic, C. Moreno-Castilla and J. Rivera-Utrilla, in: L. R. Radovic (Ed.), Chemistry and Physics of Carbon, Dekker, New York, 27 (2000).
19. C. Moreno-Castilla, *Carbon*, **42**, 83 (2004).
20. R. Coughlin and F. S. Ezra, *Environ. Sci. Technol*., **2**, 291 (1968).
21. J. S. Mattson, J. H. B. Mark, M. D. Malbin, J. W. J. Weber and J. C. Crittenden, *J. Colloid Interface Sci*., **31**, 116 (1969).
22. L. Li, P. A. Quinlivan and D. R. U. Knappe, *Carbon*, **40**, 2085 (2002).
23. M. Franz, H. A. Arafat and N. G. Pinto, *Carbon*, **38**, 1807 (2000).
24. S. Haydar, M. A. Ferro-Garcia, J. Rivera-Utrilla and J. P. Joly, *Carbon*, **41**, 387 (2003).
25. P. Pendleton, S. H. Wong, R. Schumann, G. Levay, R. Denoyel and J. Rouquerol, *Carbon*, **35**, 1141 (1997).
26. C. Moreno-Castilla, J. Rivera-Utrilla, M. V. López-Ramón and F. Carrasco-Marín, *Carbon*, **33**, 845 (1995).
27. Y. Shao, L. Wang, J. Zhang and M. Anpo, *Micropor. Mesopor. Mater*., **109**, 20835 (2005).
28. P. A. Bazuła, A. H. Lu, J. J. Nitz and F. Schüth, *Micropor. Mesopor. Mater*., **108**, 266 (2008).
29. R. Crisafully, M. A. Milhome, R. M. Cavalcante, E. R. Silveira, D. Keukeleire and F. Nascimento, *Bioresour. Technol*., **99**, 4515 (2008).
30. Y. Xun, Z. Shu-Ping, X. Wei, C. Hong-You, D. Xiao-Dong, L. Xin-Mei and Y. Zi-Feng, *J. Colloid Interface Sci*., **310**, 83 (2007).
31. D. Savova, N. Petrov, M. F. Yardim, E. Ekinci, T. Budinova, M. Razvigorova and V. Minkova, *Carbon*, **41**, 1897 (2003).
32. A. Celzard, A. Perrin, A. Albiniak, E. Broniek and J. F. Mareche, *Fuel*, **86**, 287 (2007).
33. C. S. Azevedo Diana, J. C. S. Araujo, Bastos-Neto Moises, B. Torres, F. Jaguaribe and L. Cavalante, *Micropor. Mesopor. Mater*., **100**, 361 (2007).
34. S. Biniak, G. Szymanski, J. Siedlewski and A. Swiatkoski, *Carbon*, **35**, 1799 (1997).
35. B. Stohr, H. P. Boehm and R. Schlogl, *Carbon*, **29**, 707 (1991).
36. P. E. Fanning and M. A. Vannice, *Carbon*, **31**, 721 (1993).
37. V. Gómez-Serrano, M. Acedo-Ramos, A. J. Lopez-Peinado and C. Valenzuela-Calahorro, *Fuel*, **73**, 387 (1994).
38. C. Moreno-Castilla, F. Carrasco-Marin, F. J. Maldonado-Hódar and J. Rivera-Utrilla, *Carbon*, **36**, 145 (1998).